

A direct comparison between climb and glide dislocation velocities in an icosahedral Al-Pd-Mn quasicrystal

F. MOMPIOU† and D. CAILLARD

CEMES-CNRS, BP4347, F-31055 Toulouse Cedex, France

[Received in final form 9 September 2004 and accepted 14 September 2004]

ABSTRACT

The formation and evolution of a dislocation dipole has been recorded during an *in-situ* heating experiment in a transmission electron microscope (TEM) at 740°C. The formation took place by pure climb in parallel planes but no subsequent annihilation was observed. Since annihilation was only possible by glide, this situation indicates that glide in two-fold planes is a considerably more difficult process than climb, at least at high temperature.

§ 1. INTRODUCTION

Since it has been proved that dislocations are responsible for plastic deformation in quasicrystals, they were assumed to move by glide, at least in icosahedral AlPdMn above the brittle-ductile transition temperature ($T > 600^\circ\text{C}$). Several glide models (Feuerbacher *et al.* 1997, Takeuchi *et al.* 1997) have been proposed but none of them has been confirmed experimentally, mainly because of a lack of a complete simultaneous determination of Burgers vector and corresponding motion plane. Aside from the glide assumption, more recent experimental results have shown that climb is probably the main mode of dislocation motion in quasicrystals between 300°C and 750°C (Caillard *et al.* 1999, 2000, 2002a, b, 2003, Mompiou *et al.* 2003, 2004). Nowadays, although a large number of authors agree that climb in quasicrystals plays a key role, several of them consider that it does not control the mobility of the dislocations but only recovery processes (Messerschmidt *et al.* 2003). Thus the question of the relative importance of climb and glide in quasicrystal plasticity is still open. A new *in-situ* experiment that gives an answer to this question is described here.

§ 2. EXPERIMENTAL

A single quasicrystalline icosahedral Al_{70.1}-Pd_{20.4}-Mn_{9.5} sample, produced by the Czochralski technique at the Institut für Festkörperforschung, Jülich, was investigated. Slices were cut out of a single grain by spark cutting. The specimens for TEM investigations were prepared by subsequent grinding, polishing and wet-chemical thinning. The sample normal is parallel to a pseudo two-fold direction [2/1, 1/2, 1/1] (CSG indexing of Cahn *et al.* 1989).

†Author for correspondence. Email: mompiou@cemes.fr

Table 1. Contrast conditions for one of the dipole dislocations with Burgers vector $\mathbf{b}_{//} = a_0[4/2, 2/2, 0/0]$, or $\mathbf{B} = A_0(3\bar{1}\bar{1}\bar{1}1)$. E=extinction, D=double contrast and WE=weak extinction.

\mathbf{g}	$\mathbf{g}_{//}$	\mathbf{G}	G.B	figure 2
$\mathbf{g}_{2a(1)}$	$2/3, \bar{1}/2, 1/1$	$020\bar{2}11$	0	a (E)
$\mathbf{g}_{2a(2)}$	$3/5, 2/3, 1/2$	$030\bar{3}22$	0	
$\mathbf{g}_{2b(1)}$	$1/2, \bar{1}/1, 2/3$	021102	0	b (E)
$\mathbf{g}_{2b(2)}$	$2/3, \bar{1}/2, 3/5$	$032\bar{2}03$	0	
$\mathbf{g}_{2c(1)}$	$1/2, 1/1, 2/3$	$10\bar{1}0\bar{2}\bar{2}$	0	c (WE)
$\mathbf{g}_{2c(2)}$	$2/3, 1/2, 3/5$	$20\bar{2}03\bar{3}$	2	d (D)
$\mathbf{g}_{2d(1)}$	$1/1, 2/3, 1/2$	$1\bar{1}020\bar{2}$	0	e (WE)
$\mathbf{g}_{2d(2)}$	$1/2, 3/5, 2/3$	$2\bar{2}030\bar{3}$	2	f (D)
\mathbf{g}_{5a}	$0/0, 1/2, 2/3$	$1\bar{1}\bar{1}112$	1	g

The sample was heated in a JEOL 2010 HC transmission electron microscope operated at 200 kV. The temperature was high enough (730°C and 740°C at the sample level) to activate dislocation motion under thermal and internal stresses developed in the foil. Dynamic sequences were recorded by a video camera. The planes of motion were determined by their trace directions and the variation of their apparent widths as a function of the specimen tilt angle. For subsequent contrast analysis, including Burgers vector characterization, the sample could be rapidly cooled to room temperature within 10 s. This allowed maintenance of the high-temperature configuration. Diffraction patterns taken during and after heating unambiguously showed that the icosahedral structure was maintained during the experiment, which was carried out rapidly enough to avoid excessive sample degradation. Dislocations were imaged under two-beam conditions using diffraction vectors along five-fold and two-fold directions, noted \mathbf{g}_{5i} , $\mathbf{g}_{2i(1)}$ and $\mathbf{g}_{2i(2)}$, respectively, where $\mathbf{g}_{2i(c)} = \tau \mathbf{g}_{2i(1)}$ (τ is the golden mean). The diffraction vectors, \mathbf{g} , in the physical space, expressed in the CSG notation, and the corresponding vectors, \mathbf{G} , in six-dimensional space, are given in table 1. Details on the dislocation contrast analysis can be found in Wollgarten *et al.* (1991) and Momprou *et al.* (2003).

§ 3. OBSERVATIONS

Figure 1 has been extracted from a video sequence of two dislocations (d_1 , d_2) moving in a five-fold plane P_A at 730°C (see the stereographic projection in figure 3). The dislocations are made of three straight segments oriented along two-fold directions (\mathbf{u}_1 , \mathbf{u}_2 , \mathbf{u}_3), a situation that is typical of dislocation motion in five-fold planes (Momprou *et al.* 2004). After a few seconds, the two dislocations interact and eventually annihilate (see figure 1c), as is the case for dislocations with opposite Burgers vectors in ordinary crystals. The remaining contrast, due to traces of motion at the surface, does not evolve subsequently (figure 1d). The perfect alignment of the traces shows that the two planes were identical or very close to each other.

A very different situation is shown in figure 2, where two dislocations (d_3 , d_4) moving toward each other in five-fold planes P_B , at 740°C, do not annihilate. Here too, the dislocations appear as two straight segments oriented along a two-fold direction (\mathbf{u}_5), leaving straight traces of motion at the sample surfaces (tr. P_B) which do not disappear during the experiment. The final configuration (D) remains

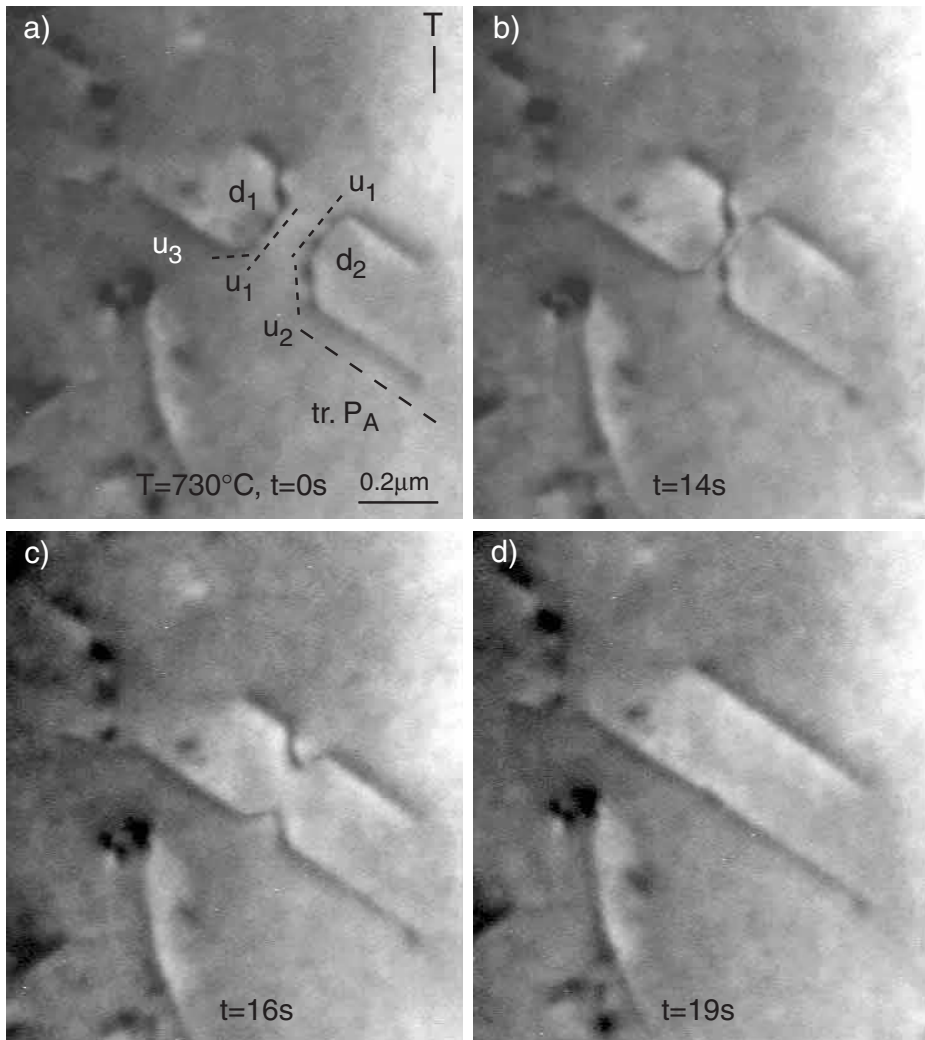


Figure 1. Dynamic sequence showing the annihilation of two opposite dislocations (d_1 , d_2) moving in a common 5-fold plane (P_A) at 730°C .

stable even after additional heating several tens of minutes, whereas other dislocations still move and eventually stop when the driving stress decreases. In both cases, no phason faults are visible in the wake of the dislocations, as expected considering the easy phason dispersion at high temperature and the low dislocation velocity (Mompiau *et al.* 2004).

To understand the difference in behaviour between the two cases, we performed a detailed analysis of the second one with the following results. The actual final configuration is made of the two dislocations aligned along the pseudo-two-fold direction \mathbf{u}_4 . Note that the intensity of the contrast of the resulting configuration (D) is smaller than the global intensity of the two original dislocations. This is typical of dislocation dipoles where the elastic fields coming from the individual dislocations partly compensate each other.

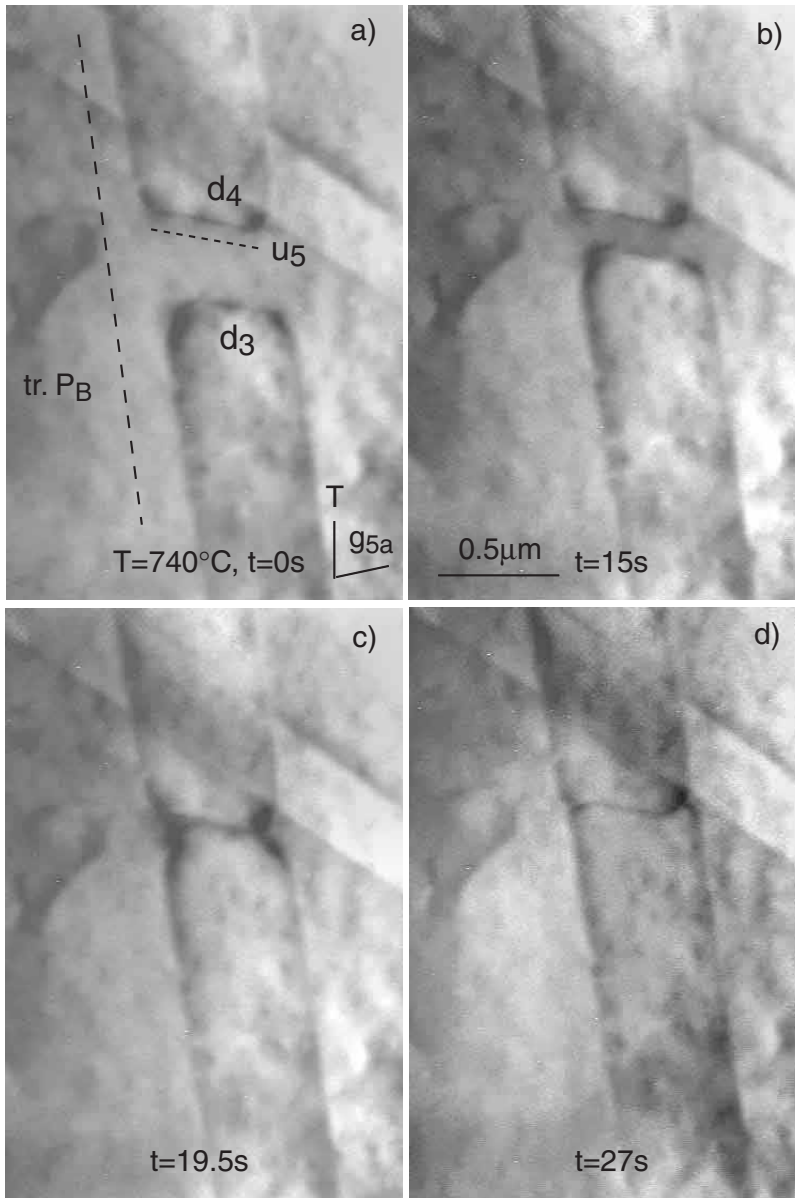


Figure 2. Dynamic sequence showing two opposite dislocations (d_3 , d_4) moving in closely parallel 5-fold planes (P_B) at 740°C . The dislocations interact in (c) and form a stable dipole in the direction u_4 in (e).

An enlarged view of the dislocation dipole is shown in figure 4. The dipole has been imaged in the $+g_{5a}/-g_{5a}$ conditions, under similar excitation errors, and under three different inclinations with respect to the electron beam. A dipolar effect arises when the plane, noted P_C in figure 3, is inclined at an angle $i = \pm 12^\circ$. In the first case ($i = 12^\circ$) two faint contrasts and a single strong contrast can be observed for g_{5a} and $-g_{5a}$, respectively (figures 4a and 4b). In the second case, the situation is reversed with a single contrast in figure 4e and a double contrast in figure 4f. In the situation

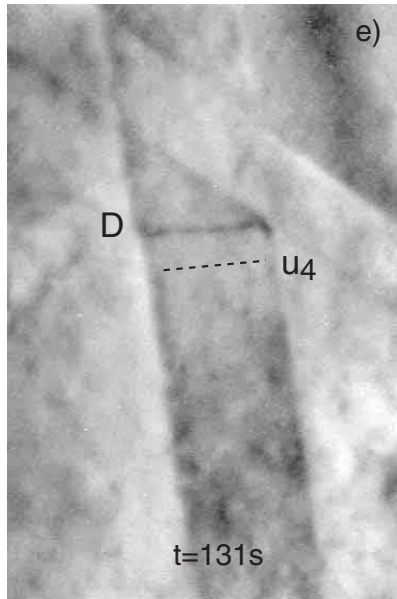


Figure 2. Continued.

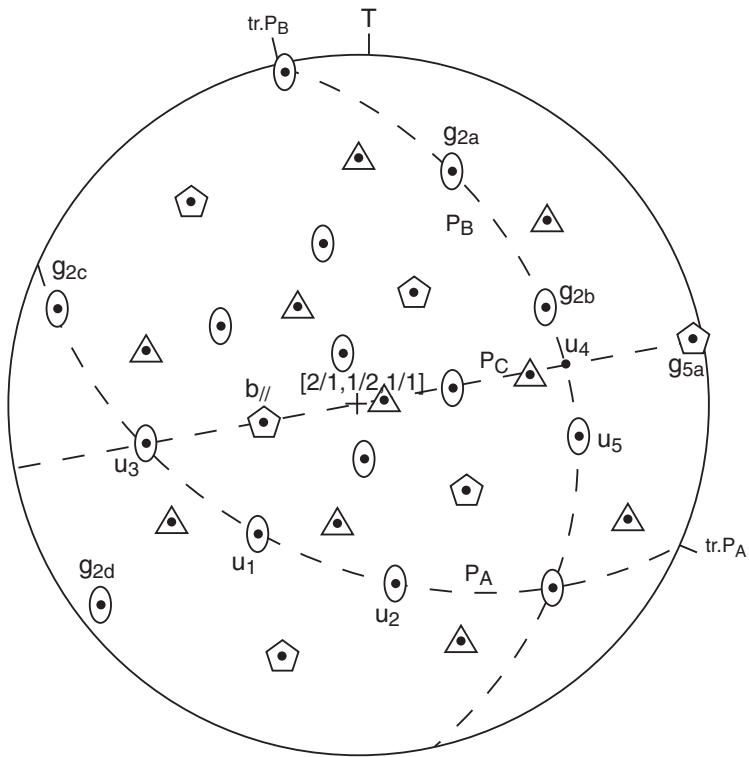


Figure 3. Stereographic projection of the observed sample. T refers to the tilt axis.

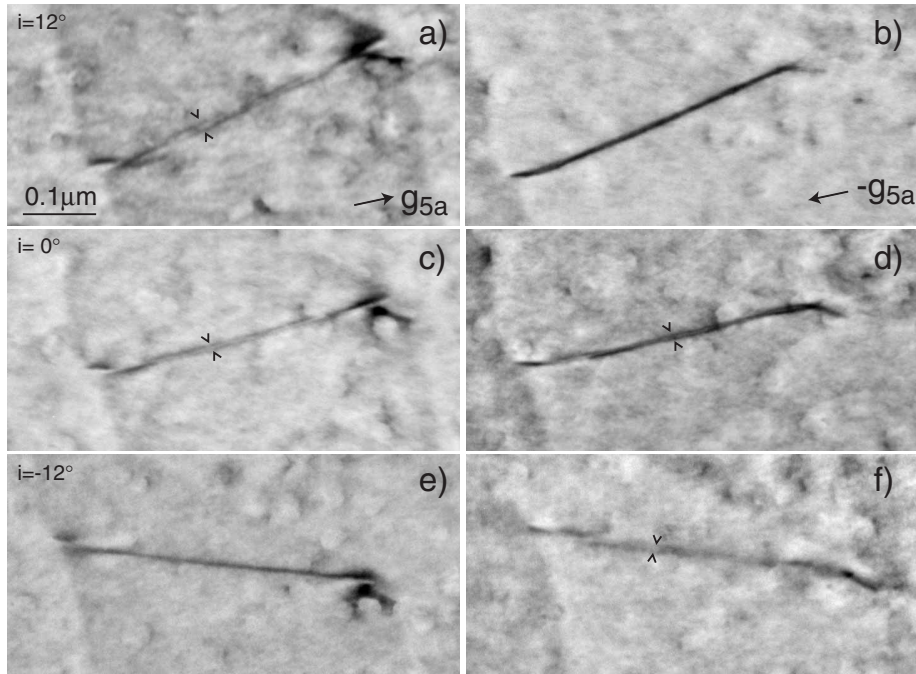


Figure 4. Dislocation dipole imaged under $\pm g_{5a}$ conditions and different inclinations.

where the plane P_C is not inclined ($i=0^\circ$), both images exhibit a double contrast (figures 4c and 4d).

This contrast can be explained as follows. The shift between the images and the real positions of the dislocations is such that the images can overlap only when the dipole plane is inclined with respect to the electron beam, for a given sign of g_{5a} . Double contrast is obtained in all other situations, including when the dipole plane is parallel to the electron beam. In the latter case, the positions of the two images are exchanged when the sign of g_{5a} is reversed. These results show that the dipole plane is almost perpendicular to the foil plane, namely close to the two-fold plane P_C .

Strong extinction conditions have been realized in $g_{2a(1)}$, $g_{2a(2)}$ (figure 5a) and $g_{2b(1)}$, $g_{2b(2)}$ (figure 5b). The dislocations are also out of contrast in $g_{2c(1)}$ (figure 5c) and $g_{2d(1)}$ (figure 5e). Since they are clearly visible for the τ -times larger diffraction vectors $g_{2c(2)}$ and $g_{2d(2)}$ (figures 5d and 5f), these situations correspond to “weak” extinctions. It can be noted that traces of motion are out of contrast in strong extinction conditions whereas they remain visible in weak extinction ones. This can be simply understood if we assume that the contrast of the traces is mostly due to elastic relaxation at the surfaces, whereas the contrast of perfect dislocations arises from both elastic and phason fields. Although the dislocations are very close to each other, a double contrast can be observed for one of them, in a region where they are separated, in $g_{2c(2)}$ (see arrowheads in the inset figure 5d) and probably in $g_{2d(2)}$ although the contrast is not completely clear (figure 5f). A single contrast in g_{5a} (figure 5g) completes the observations.

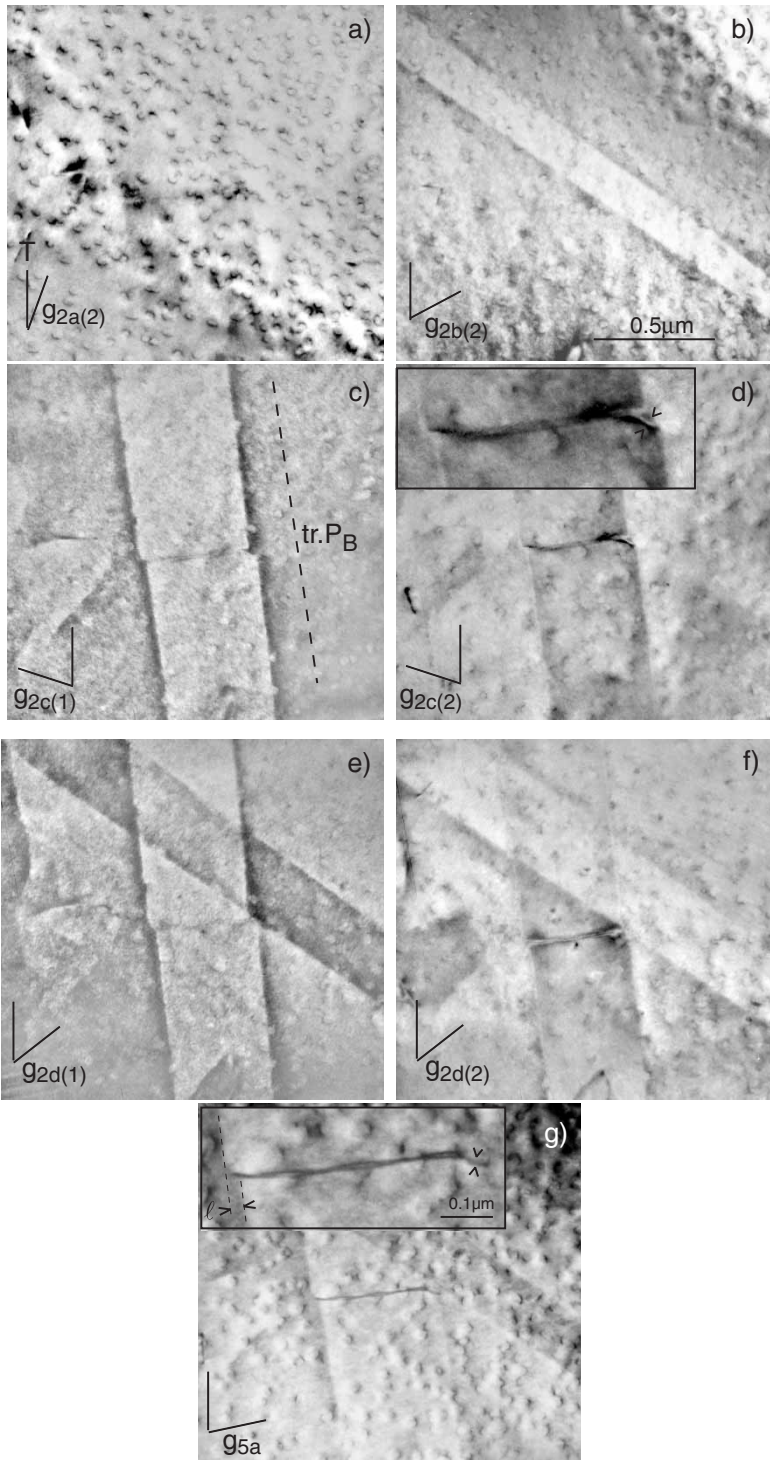


Figure 5. Contrast analysis of the dislocation dipole. Note weak extinction conditions in (c), (e) and double contrast conditions in (d) and maybe in (f). Note the shift (l) in trace directions in the inset in (g).

All the contrast conditions are summarized in table 1 and lead to a five-fold Burgers vector, $\mathbf{B} = A_0[3\bar{1}\bar{1}\bar{1}1]$ ($A_0 = 0.645$ nm is the hyperlattice constant (Boudard *et al.* 1992)), with $\mathbf{b}_{//} = a_0[4\sqrt{2}, 2\sqrt{2}, 0/0]$ of length 0.348 nm, in projection in the physical space ($a_0 = A_0/\sqrt{2(2+\tau)}$). These results are corroborated by the contrast analysis of an isolated dislocation moving on the same plane at the same time. We can conclude here that, since the Burgers vector is perpendicular to the plane of motion P_B , the dislocations have moved by pure climb. Similar climbing dislocations have already been observed in heating and heating-straining *in-situ* experiments between 680°C and 750°C (Momprou *et al.* 2004). However such a stable dipole formation has never been reported previously.

One can notice, in contrast with figure 1, that the dislocation traces at the surface are not strictly aligned but slightly shifted by a distance l (see the inset figure 5g), indicating that the dislocations have moved in closely parallel planes. This shift allows us to determine the distance, d , between the planes of motion, using the relation $d = l \sin \alpha$, where α is the angle between the surface and the plane of motion. Taking $l = 27$ nm and $\alpha = 27^\circ$, we find $d = 12$ nm.

§ 4. DISCUSSION

In their original climb plane of motion, the two approaching dislocations move at a velocity of about 6 nm/s. They are subjected to the driving stress, τ , present in the whole area, plus an elastic interaction stress given by

$$\tau_i = \frac{\mu b_{//}}{2\pi(1-\nu)} \frac{x(x^2 + 3d^2)}{(x^2 + d^2)^2}, \quad (1)$$

where x is the separation distance projected onto the climb plane (see figure 6). Taking $\mu = 53$ GPa at 740°C (Tanaka *et al.* 1996), $1 - \nu \cong 0.75$, $b_{//} = 0.348$ nm and $d \cong 12$ nm, the interaction stress, τ_i , amounts to 30 MPa at a distance $x = 130$ nm (case of figure 2b). It increases to a maximum of 359 MPa for $x = 8.1$ nm and rapidly decreases to zero for $x = 0$. Because of the driving stress,

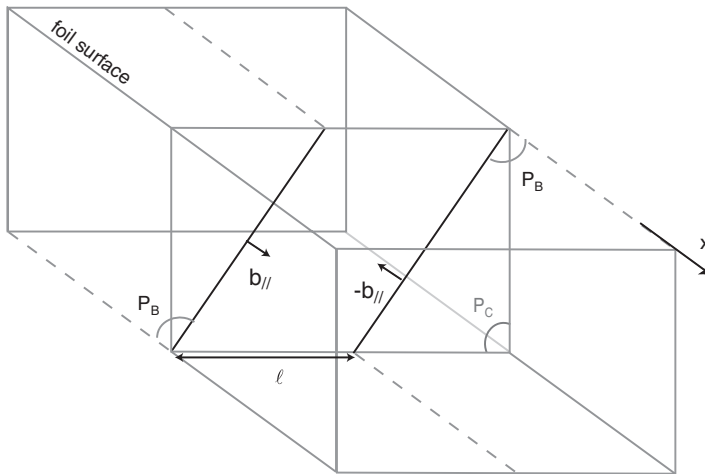


Figure 6. Schematic representation of the dipole formation.

the dislocations stop slightly beyond this position. They, however, progressively move back after relaxation of the driving stress. An estimate of the driving stress at the end of the experiment can be made as follows. When dislocation motion is not observed anymore in the thin foil, the driving stress is assumed to be lower than a few tens of MPa (which is about 1/10 of the average macroscopic stress for dislocation motion taking place at about 10 nm/s, from Feuerbacher *et al.* (1997)). The final equilibrium position of the dipole accordingly corresponds to x smaller than 1 nm. It corresponds to a dipole plane which is less than 3° from the plane P_C perpendicular to the climb plane and containing the dislocation direction \mathbf{u}_4 (figure 3), in agreement with the conclusion of the contrast analysis. This plane is the common “glide plane” for the two dislocations of the dipole.

In standard crystals this would be considered as the ideal case for dislocation annihilation by glide with an interaction stress

$$\tau_g = \frac{\mu b_{//}}{2\pi(1-\nu)d}, \quad (2)$$

which amounts to 320 MPa. It turns out that in the present case, the interacting force that is sufficient to induce rapid climb, is still not enough to induce glide! Considering that the velocity of glide is necessarily much lower than $d/t_{\text{obs}} = 6 \times 10^{-3} \text{ nm s}^{-1}$, where t_{obs} is the observation time ($t_{\text{obs}} = 1800 \text{ s}$), the velocity of glide is at most 10^{-3} lower than that of climb, under comparable stresses.

This shows that the ratio of glide, in two-fold planes, versus climb velocities, is reversed with respect to crystals where climb is usually slower than glide, even at high temperature. Contrary to this situation, the annihilation was possible in figure 1 because the two opposite dislocations were in the same climb plane. Although the Burgers vectors of dislocations in figure 1 have not been determined, we can reasonably assume that they have moved by climb as others in five-fold planes. Note that the unique observation described in this article is sufficient to prove the impossibility of glide in two-fold planes because it relates a well-defined situation recorded as a function of time. We thus conclude that climb not only controls recovery but also dislocation mobility.

Dipole formation probably contributes to hardening in Al-Pd-Mn. However, since global softening is observed instead of hardening, the latter effect appears to be negligible. This conclusion is supported by *post-mortem* observations showing 3-D dislocation networks instead of pile-ups of climbing dislocations against dipoles (Messerschmidt *et al.* 2001). As a result, dipole annihilation by glide in Al-Pd-Mn appears unnecessary to achieve large deformations, in contrast with dipole annihilation by climb in crystals, for example in the frame of the Weertman creep model (Weertman 1957a, b).

The fact that glide is definitely more difficult than climb could be supported by topological arguments. Shear along corrugated worms (the equivalent of dense planes in quasicrystals) indeed destroys locally the topology of the structure (Mikulla *et al.* 1995). On the contrary, motion by pure climb, which induces displacement perpendicular to the worms, although introducing phason faults, would preserve the topology of the structure (Caillard *et al.* 2003).

§ 5. CONCLUSIONS

The formation and the evolution of a dislocation dipole in Al-Pd-Mn at 740°C has been observed in TEM during an *in-situ* heating experiment. Contrast and kinetics analyses have shown that:

- (i) the dipole forms by pure climb;
- (ii) the dipole does not evolve significantly although it could annihilate by glide in a two-fold plane.

From these observations, it is concluded that high-temperature glide in a two-fold plane is a process which is a thousand times slower than climb under similar stresses.

ACKNOWLEDGEMENTS

The authors are indebted to M. Feuerbacher for supplying samples and to M. Feuerbacher and D. Gratias for fruitful discussions.

REFERENCES

- BOUDARD, M., DE BOISSIEU, M., JANOT, C., HEGER, G., BEELI, C., NISSEN, H. U., VINCENT, H., IBBERTSON, R., AUDIER, M., and DUBOIS, J. M., 1992, *J. Phys. cond. Matter*, **50**, 10149.
- CAILLARD, D., MOMPIOU, F., BRESSON, L., and GRATIAS, D., 2003, *Scripta mater.*, **49**, 11.
- CAILLARD, D., MORNIROLI, J. P., VANDERSCHAEVE, G., BRESSON, L., and GRATIAS, D., 2002a, *Eur. Phys. J. AP*, **20**, 3.
- CAILLARD, D., ROUCAU, C., BRESSON, L., and GRATIAS, D., 2002b, *Acta mater.*, **50**, 4499.
- CAILLARD, D., VANDERSCHAEVE, G., BRESSON, L., and GRATIAS, D., 1999, *Mater. Res. Soc. Symp. Proc.*, **553**, 301; 2000, *Phil. Mag. A*, **80**, 237.
- CAHN, J. W., SHECHTMAN, D., and GRATIAS, D., 1989, *J. Mater. Res.*, **1**, 13.
- FEUEURBACHER, M., METZMACHER, C., WOLLGARTEN, M., BAUFELD, B., BARTSCH, M., MESSERSCHMIDT, U., and URBAN, K., 1997, *Mater. Sci. Engng A*, **233**, 103.
- MESSERSCHMIDT, U., and BARTSCH, M., 2003, *Scripta mater.*, **49**, 33.
- MESSERSCHMIDT, U., PETRUKHOV, B. V., BARTSCH, M., DIETZSCH, CH., GEYER, B., HAÜSLER, D., LEDIG, L., FEUEURBACHER, M., SCHALL, P., and URBAN, K., 2001, *Mater. Res. Engng A*, **319–321**, 107.
- MIKULLA, R., ROTH, J., and TREBIN, H.-R., 1995, *Phil. Mag. B*, **5**, 981.
- MOMPIOU, F., BRESSON, L., CORDIER, P. and CAILLARD, D., 2003, *Phil. Mag.*, **83**, 3133.
- MOMPIOU, F., FEUEURBACHER, M., and CAILLARD, D., 2004, *Phil. Mag.*, **84**, 2772.
- TAKEUCHI, S., SHINODA, K., and EDAGAWA, K., 1997, *Phil. Mag. A*, **79**, 317.
- TANAKA, K., MITARAI, Y., and KOIWA, M., 1996, *Phil. Mag. A*, **73**, 1715.
- WEERTMAN, J., 1957a, *J. appl. Phys.*, **28**, 362; 1957b, *ibid.*, **28**, 1185.
- WOLLGARTEN, M., GRATIAS, D., ZHANG, Z., and URBAN, K., 1991, *Phil. Mag. A*, **64**, 819.